

Cyclosporin A (10 mg/kg body weight) was subcutaneously administered for 2 weeks for immunosuppression.

Evaluation

Radiographic Measurement of Disc Height Index. Lateral radiographs of the lumbar spine (60 kV, 10 mA, distance 100 cm) were taken just before aspiration of the NP and at 0, 2, 4, 6, 10, 18, and 26 weeks after the first operation with 3 rabbits from randomly selected. To avoid axial rotation of the spine and decrease the error from beam divergence, fluoroscopic control was used and radiographs were repeated twice for each animal, with the beam center located 5 cm from the iliac crest. These radiographs were digitally scanned and stored in a computer. Using digitized radiographs, the vertebral body and IVD heights were measured using image software (J image, NIH) the disc height index (DHI) at each level was determined based on the method of Lu *et al.*²¹ Changes in the DHI were expressed as %DHI and normalized to the measured preoperative IVD height ($\%DHI = \text{postoperative DHI}/\text{preoperative DHI} \times 100$, Figure 1).

Macroscopic and Histologic Examination. At 6, 10, and 26 weeks after the first operation, 4 rabbits from each group, a total of 12 rabbits at each time point, were killed by intravenous injection of high-dose pentobarbital sodium (120 mg/kg, Abbott). The L2–L3, L3–L4, and L4–L5 discs were excised immediately in continuity with their cranial and caudal vertebral bodies. These columnar tissues were removed, muscles and nerves were cut off, and the vertebral body–disc–vertebral body units were separated ($n = 3$ discs from each rabbit, a total of 12 discs per group). The units were then fixed in 10% neutral buffered formalin solution (Wako), decalcified in Plank–Rychlo solution (Decalcifying Solution A; Wako), dehydrated in a graded series of ethanol (70%, 90%, 99%, Wako), and processed individually for paraffin wax embedding. To evaluate gross findings, photographs were taken from sagittal plane of the remaining tissues. The paraffin blocks were sectioned longitudinally using a microtome to give 4- μm sections. The center of the outer anulus fibrosus was marked before paraffin embedding to ensure that only the center of the disc was made in to sagittal sections. The paraffin sections were dewaxed with xylene and ethanol, washed with PBS, and stained with hematoxylin and eosin, and Safranin-O for evaluation. The disc degeneration grading system of Nishimura and Mochida,¹⁰ focusing on the morphologic changes in the anular structure, was used for evaluation: Grade 0, normal structure; Grade 1, mildly serpentine appearance of the anulus fibrosus with rupture; Grade 2, moderately serpentine appearance of the anulus fibrosus with rupture; Grade 3, severely serpentine appearance of the anulus fibrosus with mildly reserved contour; Grade 4, severely reserved contour; Grade 5, indistinct. Two histologists who are familiar with human and animal IVD specimens performed evaluation of these sections, with their intraobserver error being minimum. When intraobserver discrepancies were detected, another histologist was asked to determine the grade (agreement between observers was 96.3%).

Immunohistochemistry. Proteoglycan staining changes in the discs were studied to evaluate disc degeneration. After dewaxing and subsequent PBS washing, blocking of nonspecific antigen reactivity with 5% normal goat serum for 30 minutes and internal peroxidase reactivity by 3% H_2O_2 in H_2O at



Figure 1. Disc height was expressed as disc height index (DHI) based on the method described by Lu *et al.* Value in the diagram is presented as %DHI, which is obtained by dividing the DHI value obtained at the time of evaluation with DHI value obtained before the procedure. $DHI = (c + d)/(a + b)$; $\%DHI = \text{postoperative DHI}/\text{preoperative DHI} \times 100$.

room temperature for 5 minutes was performed. Next, the sections were labeled overnight at 4 C with anti-human proteoglycan monoclonal antibody (Chemicon, Temecula, CA), prepared at a dilution of 1:200 in PBS. This antibody recognizes short peptides substituted with keratan sulfate sidechains and core proteins of proteoglycans in the articular cartilage of human and rabbits. The samples were washed three times with PBS and incubated with anti-mouse horseradish peroxidase (Dako A/S, Profuktionsvej, Denmark) at a dilution of 1:100 in PBS for 30 minutes at 4 C. Furthermore, regarding Type II collagen, sections were pretreated with 0.05% protease (Sigma Chemical Co., St Louis, MO) at 37 C for 30 minutes. Antihu-

man Type II collagen antibody (Lab Vision, Fremont, CA) prepared at a dilution of 1:50 in PBS, and the sections were labeled for 30 minutes at room temperature. The samples were washed with PBS and reacted with anti-mouse HRP (Dako A/S, Profuktionsvej, Denmark) at room temperature for 30 minutes, washed and reacted with Histofine Simple Stain Diaminobenzidine (Nichirei Corp.) for 5 minutes. Finally, the sections were counterstained with hematoxylin for examination.

Survival of Transplanted Cells. To obtain frozen sections of the HNPSV-5 transplanted discs, 2 HNPSV-5 transplanted rabbits were separately made and killed 4 and 24 weeks posttransplantation. To confirm the survival of transplanted cells after transplantation, 3 discs from 1 rabbit were excised immediately in continuity with their cranial and caudal vertebral bodies at each time points. The vertebral body-disc-vertebral body units were rapidly frozen at -80°C . These discs were sectioned axially at the central level of the disc, and all samples were embedded in optimal cutting temperature compound (Tissue-Tek 4583, Sakura Finetek, Tokyo, Japan). The blocks were sectioned at $7\ \mu\text{m}$ using a cryomicrotome, and the sections were fixed in 4% paraformaldehyde at 4°C for 30 minutes and stained overnight at 4°C with mouse anti-SV40 T antigen antibody (Pab419; Oncogene, Boston, MA) diluted 1:100 in PBS with 5% normal goat serum. Goat anti-mouse IgG Alexa fluor 594 (Molecular Probes, Eugene, OR) diluted 1:50 in PBS was used as second antibody. Nuclear staining was then performed by using mounting medium containing DAPI (Vectashield, Vector, Burlingame, CA). After PBS washes, fluorescent microscopic evaluation was performed to assess the percentage of double positive cells in the NP.

Graft-Versus-Host Reaction in Transplanted Discs. Frozen sections of HNPSV-5-transplanted rabbit discs harvested at 4 weeks and 24 weeks after transplantation were used for evaluation of the presence of graft-versus-host reaction. The mesenteric lymph nodes were also excised and were rapidly frozen at -80°C for control samples. The sections were pretreated with a blocking buffer (10% normal goat serum in $1 \times \text{PBS}$) for

15 minutes. Purified mouse anti-rabbit CD4 monoclonal antibody (lot: M042011, BD) and CD58 monoclonal antibody (lot: 0296-0698, VMRD, Inc.) were prepared at 1:50 dilution in PBS, and sections were labeled overnight at 4°C . The samples were washed with PBS and reacted with Histofine Simple Stain Peroxidase (Nichirei Corp., Tokyo, Japan) for 60 minutes at room temperature and Histofine Simple Stain Diaminobenzidine (Nichirei Corp.) for 5 minutes. Finally, the sections were counterstained with hematoxylin for immunohistochemical examination.

Reverse Transcription-Polymerase Chain Reaction. At 26 weeks after the first operation, total RNA was extracted from the discs in three groups (2 rabbits, 6 discs from each group) using Isogen reagent (Nippon Gene, Tokyo, Japan). RNA samples were then reverse transcribed to cDNA using oligo dT primers and Multiscribe Reverse transcriptase (Applied Biosystem, Foster City, CA), followed by specific amplification of matrix specific genes and electrophoretic separation. Gene specific PCR primers were designed using rabbit mRNA sequence data obtained from GenBank, which is shown as follows: Aggrecan: $5' - \text{GAGGAGATGGAGGGT-GAGGTCTTT} - 3'$, $5' - \text{CTTCGCCTGTGTAGCAGCTG} - 3'$; versican: $5' - \text{TTATGTGGATCATCTGGACGG} - 3'$, $5' - \text{GCA-TCCAAGAGCCACCCA} - 3'$; Type II collagen: $5' - \text{AACACTGCC-AACGTCCAGAT} - 3'$, $5' - \text{CTGCAGCACGGTATAGGTGA} - 3'$; GAPDH: $5' - \text{TCACCATCTTCCAGGAGCGA} - 3'$, $5' - \text{CACAA-TGCCGAAGTGGTCGT} - 3'$. The gels were scanned under UV light with a Densitograph system (Atto Biotechnologies inc, Tokyo, Japan) and band intensities were quantified densitometrically and normalized to GAPDH gene values using a CS Analyzer (version, 2.01, Atto).

Statistical Analysis. Comparison of group means between NC, DG, and Tx groups were determined using the repeated measure ANOVA and fisher's PLSD *post hoc* test. Statistical significance was determined based on $P < 0.01$. Error bars were set to represent standard deviation (SD).

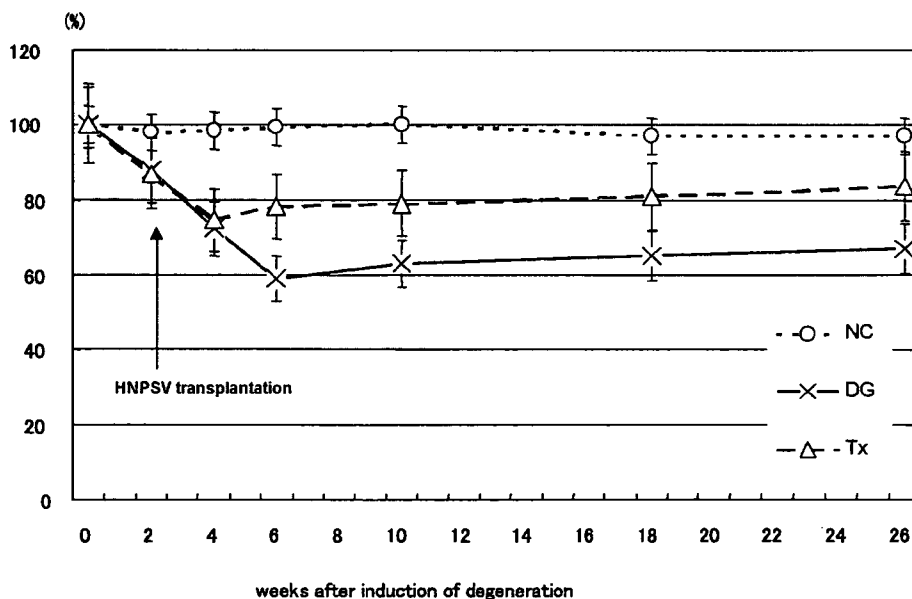


Figure 2. Decrease of %DHI in DG and Tx groups begun at 2 weeks after the first operation. After 4 weeks, there was significant statistical difference between DG and Tx group discs compared with NC group discs. (NC, 98.5 ± 7.60 ; DG, 72.29 ± 9.38 ; Tx, 74.55 ± 6.61 , $P < 0.001$). %DHI of Tx group at 4 weeks after HNPSV-5 transplantation recovered significantly (NC, 99.4 ± 6.04 ; DG, $59.1 \pm 6.49\%$; Tx, $78.01 \pm 8.76\%$, $P < 0.001$).

■ Results

Disc Height Change Measured by DHI

Two weeks after nucleus aspiration, a significant decrease in the disc height measurement was detected in both the DG and Tx groups. In the Tx group, the %DHI began to return towards normal from 2 weeks after transplantation. At 4 weeks after transplantation, the %DHI of the Tx group was significantly higher than that of the DG group (DG: $59.1\% \pm 6.49\%$; Tx: $78.01\% \pm 8.76\%$). The NC group maintained a %DHI of $97.1\% \pm 7.23\%$ throughout the 26 weeks. At 24 weeks after transplantation, the %DHI of the Tx group was significantly higher than that of the DG group (DG: $66.87\% \pm 8.35\%$; Tx: $83.69\% \pm 7.03\%$), showing the effectiveness of HNPSV-5 transplantation (Figure 2).

Macroscopic Examination

Nucleus pulposus in NC group's discs showed NP with containing ovalshaped gelatinous tissue with distinct structure of nucleus-anulus border (Figure 3a). At 26 weeks after nucleus aspiration, discs in the DG group showed depletion of the nucleus, in which the nucleus-anulus border could not be identified, with a significant decrease in disc height compared with NC group's discs (Figure 3b). In the discs of the Tx group, the NP could be found, but not as perfectly oval shaped as NC group's discs, but apparent border between the NP and the anulus fibrosus (AF) could be identified (Figure 3c).

Histologic Analysis

Discs of NC group rabbits did not show significant degenerative changes throughout all the experimental period (Figure 4a, b). In the discs of DG group's rabbits, at 10 weeks after the first operation, the NP cells remained with demonstrating some cell clumping and disintegration of the curved structure of the inner AF. At 26 weeks after the operation, the structural appearance of the nucleus tissue disappeared with apparent invasion of surrounding connective tissue and the curved structure of AF had completely collapsed (Figure 4c, d).

In the HNPSV-5-transplanted model, the structure of the NP and AF was maintained throughout the experiment. However, mild degenerative changes, such as the mild serpentine appearance of AF, were seen from 6 weeks after nucleus aspiration. The NP of the Tx group's discs did not show histologic appearances similar to the normal rabbit discs. Instead, honeycomb appearances with slight proliferation of surrounding connective tissue were noted. As for presence of tumorigenesis, invasion of transplanted cells from the nucleus to anulus or the cartilage endplate was not found 24 weeks after transplantation (Figure 4e, f).

In analysis performed 6, 10, and 26 weeks after nucleus aspiration using the histologic grading system, grading of the discs from DG group consistently moved toward higher grade with time (Figure 5). At 26 weeks, 83.3% of the DG group's discs were Grade 5, whereas in

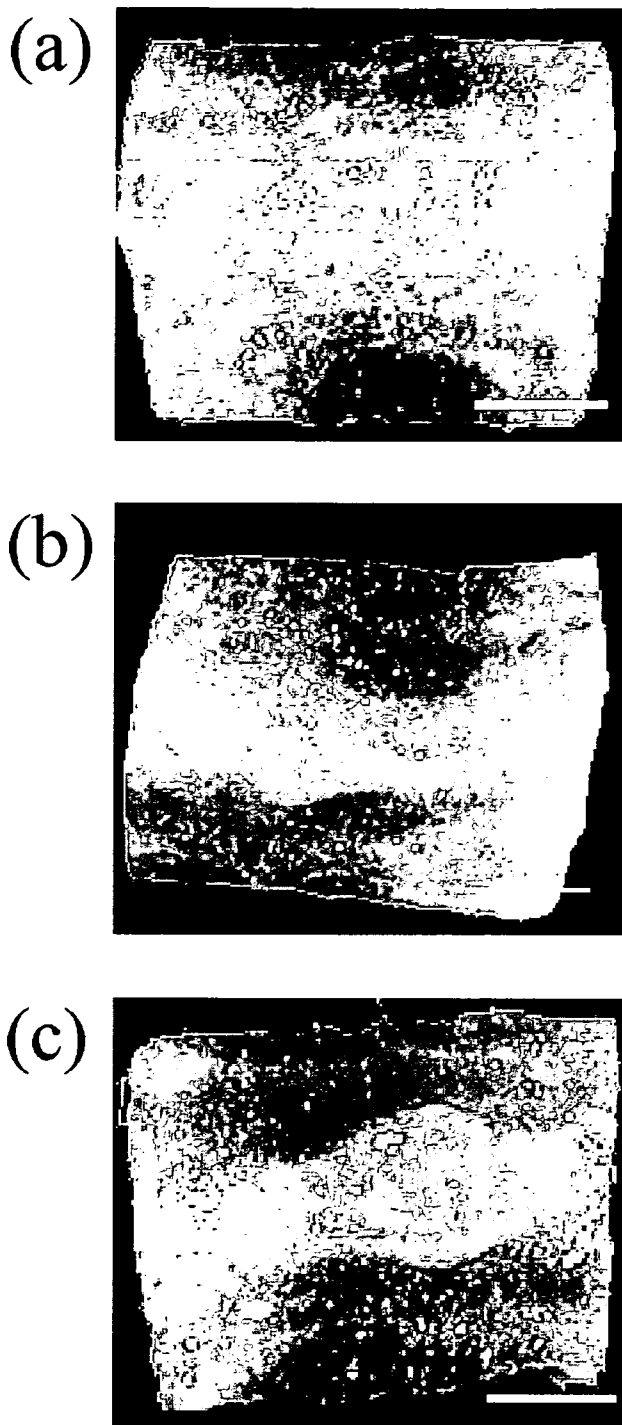


Figure 3. a, In macroscopic findings, NC group's disc showed intact oval-shaped gel-like nucleus. b, DG group discs presented narrowing of disc height and absence of the nucleus pulposus. c, Although not perfectly circular, restoration of nucleus and recovery of disc height were achieved by HNPSV-5 transplantation. Bars = 2 mm.

the Tx group's discs, 66.7% were Grade 2 and 25% Grade 3, which clearly shows that cell transplantation significantly decelerated disc degeneration in the Tx group's discs in comparison with the DG group's discs (Figure 5c).

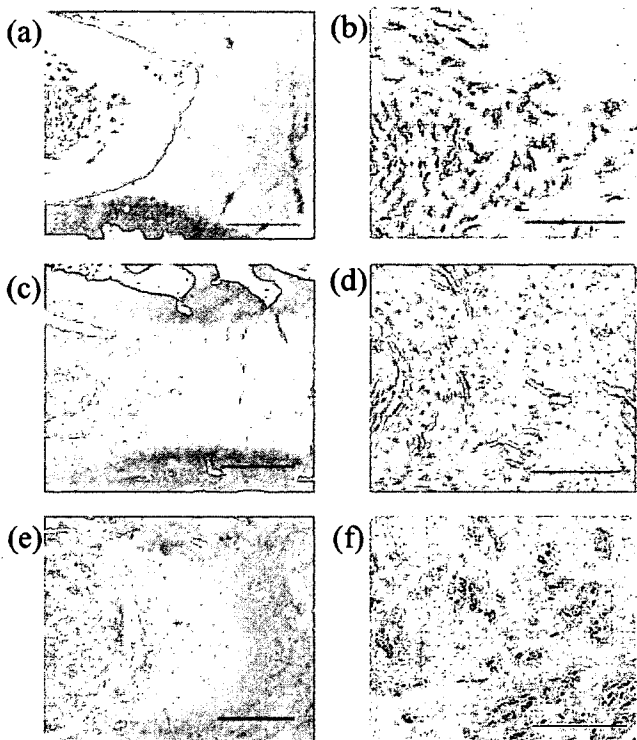


Figure 4. **a** and **b**, Sagittal section of NC group's disc (age equivalent to 26 weeks after the first operation in the other groups) with the majority of the cells composing the nucleus being large vacuolated cells in spatial gelatinous extracellular matrix. Grade 0, normal structure. **c** and **d**, Discs of DG group's disc group rabbits 26 weeks after the first operation. Completely ruptured or reversed lamellar fibers and invasion of connective tissue is present, which is graded as Grade 5, indistinct structure. The HNPSV-5 transplanted disc figures (**e** and **f**) show moderately serpentine appearance of the inner anulus fibrosus, Grade 2, and in the nucleus, chondrocyte-like cells in honeycomb appearance showing a mildly DG group's disc. Bars = 500 μ m (**a**, **c**, **e**), 200 μ m (**b**, **d**, **f**).

Safranin-O, Proteoglycan Staining, and Type II Collagen Staining

The staining intensity of Safranin-O and proteoglycan in the NC group's discs was most strongly stained among the discs of the three groups (Figure 6a, b). At 24 weeks after transplantation, in the DG group's discs, the staining intensity of Safranin-O decreased or did not show significant intensity in the area where the NP were depleted (Figure 6a-DG). In contrast, Tx group's discs showed high Safranin-O staining intensity close to that of normal rabbit discs (Figure 6a, NC). The staining of proteoglycan was equivalent to that of Safranin-O (Figure 6b, DG and Tx). Therefore, it was suspected that the transplanted HNPSV-5 cells produced proteoglycan after transplantation. With regard to Type II collagen staining (Figure 6c), the nucleus pulposus and internal layer of the disc were strongly stained in the NC group. The DG group did not show such strong staining as the NC group. The disc was more strongly stained in the Tx group than in the DG group. The internal layer of the anulus fibrosus was more strongly stained than the outer layer in the Tx group, although the difference between the two layers was not as evident as in the NC group.

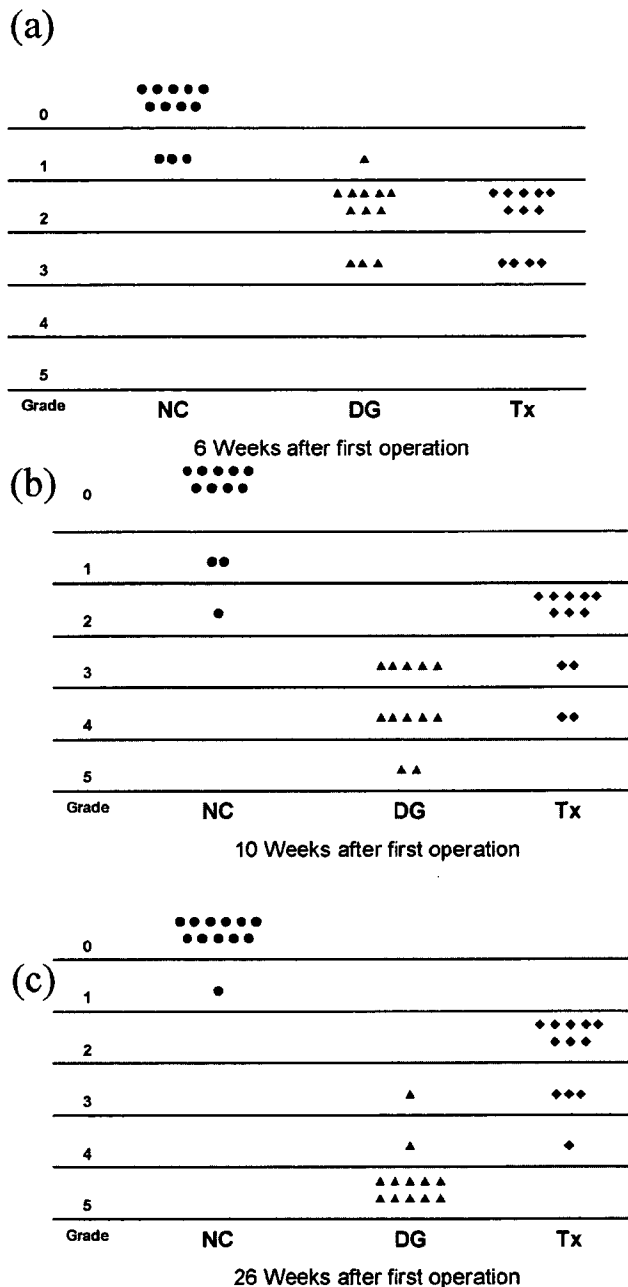


Figure 5. The results of analysis of disc degeneration using the 6-stage histologic grading system of Nishimura and Mochida. **a**, At 2 weeks after nucleus aspiration, discs of both DG and Tx group discs showed mild degenerative changes. **b**, At 10 weeks after nucleus aspiration, only discs of DG group's discs continued to progress degeneration. **c**, At 26 weeks after nucleus aspiration, 83.3% of discs from DG group's discs showed Grade 5, indistinct structure, whereas in discs of HNPSV-5 group, 66.7% preserved Grade 2 and 25% Grade 3. These findings indicate that HNPSV-5 transplantation therapy efficiently suppressed disc degeneration.

Graft-Versus-Host Reaction

The degree of immunoreaction in the Tx group's discs was quantified using anti-CD4 and CD58 monoclonal antibodies to detect an invasion of lymphocytes or monocytes (Figure 7a, b). Mesenteric lymph nodes, which stained prominently, served as the positive control

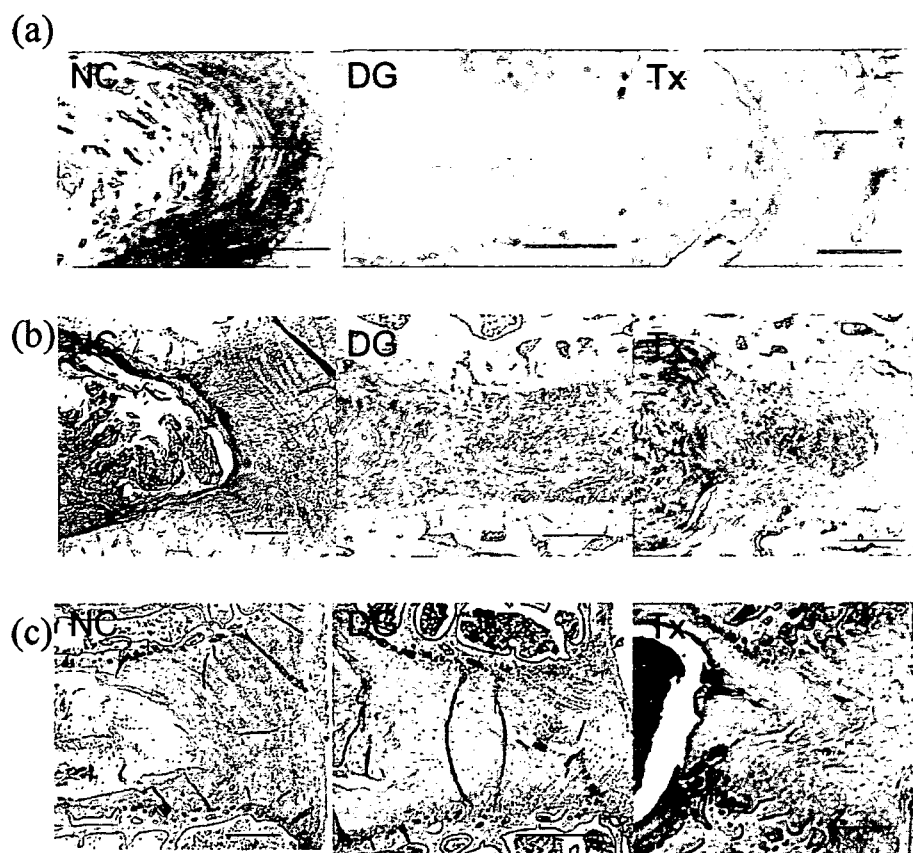


Figure 6. Staining for Safranin-O (a) and proteoglycan (b) in discs of NC group, showing strong intensity in nucleus and inner annulus. In the discs of DG group's disc, staining intensity of both Safranin-O and proteoglycan was uniform and poor. In Tx group's discs, staining was seen in both the regenerated nucleus and the inner annulus. c, Staining for Type II collagen. Bars = 500 μ m.

(Figure 7c, d). When the nucleus pulposus of the IVDs in the NC group was stained as a negative control, no positive cells were noted (Figure 7e, f). None of the sections of the Tx group's discs harvested 4 and 24 weeks after transplantation were stained by CD4 or CD58 anti-rabbit monoclonal antibody and the results demonstrated no infiltration of inflammatory cells in transplanted space.

Matrix Gene Expression

The effect of cell transplantation on the gene expression of aggrecan, versican, and Type II collagen was semi-quantified by RT-PCR, with values normalized to GAPDH. At 24 weeks after transplantation, the all mRNA expressions of were significantly enhanced by cell transplantation (aggrecan; DG: 32.01 ± 18.36 , Tx: 78.37 ± 12.3 , versican; DG: 71.95 ± 21.03 , Tx: 124.7 ± 18.6 , Type II collagen; DG: 62.09 ± 11.8 , Tx: 77.36 ± 13.6 , $P < 0.001$, Figure 8).

Survival of Transplanted Cells

Axial sections of Tx group's discs showed that average of $89\% \pm 5\%$ of cells in NP stained positive for SV40 T antigen (Figure 9). Normal rabbit discs stained as a negative control showed no positive cells. Accordingly, survival of HNPSV-5 cell line was confirmed for the 24 weeks after transplantation.

Discussion

In recent years, various different cell types have been examined as possible donor cells for IVD transplantation

therapy. Others¹⁰⁻¹² transplanted NP cells including notochord cells into IVDs of the rats and rabbits, but notochord cells are extremely uncommon in the IVDs of adult humans, with chondrocyte-like cells accounting for almost all of the cells that can be detected. To achieve the most effective tissue regeneration, it is desirable to use cellular constituents that usually form a particular tissue. However, clinical access to healthy NP tissue is very restricted, and even if tissue is obtained by some fortuitous circumstance, *in vitro* expansion is difficult.

With this in mind, Ganey *et al*⁸ and Gruber *et al*⁹ performed animal studies on the use of disc chondrocytes for transplantation. As they also transplanted cellular constituents of the AF into the NP, changes from the original tissue environment can be anticipated, and further consideration is required before this technique can be applied clinically.

Others¹³⁻¹⁵ are also investigating the use of mesenchymal stem cells as potential donor cells. However, *in vitro* methods of inducing the differentiation of stem cells into NP cells have not yet been established. The specific markers and differentiation-inducing factors for NP cells have not been identified, so transplanted cells may not differentiate into NP cells, depending on the posttransplantation cellular environment.

Accordingly, we decided to investigate a technique using a human NP cell line as the cell source for a tissue regeneration method using cellular constituents as close to the original as possible. Establishment of this cell line allowed us to effectively amplify cells that are normally very difficult to

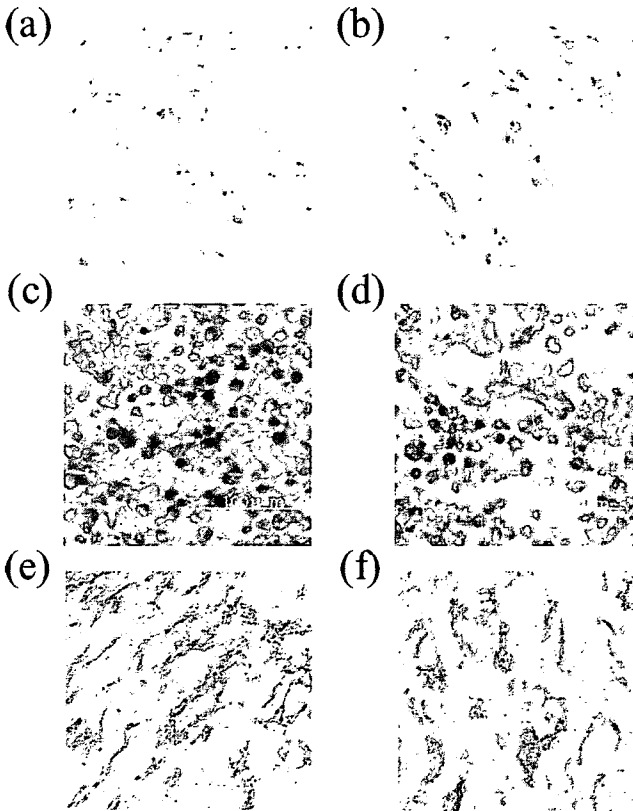


Figure 7. Immunohistochemistry results of CD4 and CD58 showed that no apparent positive staining for CD4 (a) and CD58 (b) was noted in discs of Tx group, 24 weeks after transplantation. c and d, Lymph node specimens as positive controls. e and f, Normal NP specimens as negative controls.

obtain. The HNPSV cell line that we developed uses a recombinant SV40 adenovirus vector to immortalize healthy nucleus pulposus cells, thus allowing the first *in vitro* amplification of a human nucleus pulposus cell line.¹⁹

In this study, we transplanted HNPSV cells into a rabbit IVD degeneration model and found that the disc height was significantly greater in the Tx group than in the DG group from 4 weeks posttransplantation. Macroscopically, the NP was absent in DG group at 24 weeks posttransplantation, along with the loss of disc height, whereas in the Tx group the NP was preserved. Histologic examination showed that the AF was not ruptured

in the Tx group, and the boundary between nucleus and anulus could be clearly visualized. Using the six-stage histologic grading system by Nishimura, 87% of DG group was assessed as Grade 5, whereas 67% of the Tx group was Grade 2. Expression of mRNAs for three important protein constituents of the nucleus pulposus matrix, aggrecan, versican, and Type II collagen was determined by RT-PCR, and they were significantly greater in the Tx group than in the DG group. This indicates that transplantation of HNPSV helped to preserve the matrix of the nucleus pulposus. Aguiar *et al* reported that proteoglycan synthesis by nucleus pulposus cells was increased during coculture with notochordal cells.²² It was therefore suggested that the notochordal cells derived from rabbit might interact with transplanted nucleus pulposus cells in the transplanted IVD, which might produce positive effect on degenerative IVDs. Thus, transplantation of a human NP cell line was shown to delay disc degeneration in this rabbit model.

A point that must be considered with respect to this cell transplantation model is that it involved xenograft transplantation. Accordingly, there was a risk of a graft-versus-host reaction; however, no inflammatory cell infiltration was seen through 24 weeks posttransplantation, and immunostaining revealed no cells positive for CD4 and CD58. This is thought to be because the NP maintained its immunologic integrity and because an immunosuppressant (cyclosporine) was administered at the time of transplantation. However, further long-term follow-up is required to assess rejection.

The greatest barrier to clinical application of this technique is the tumorigenic potential of transplanted cells. The HNPSV line does not proliferate unchecked *in vitro* and shows contact inhibition, with the limit of its proliferative potential being some 40 to 50 generations.¹⁹ This is because the vector is an adenovirus.²³ Unlike other viral vectors, such as retrovirus and lentivirus vectors, the adenovirus vector is not incorporated into chromosomal DNA, so expression of SV40 T antigen is transient and decreases with time.

In vivo tumorigenesis involves the unrestricted proliferation of cells and tissues but is unlike carcinogenesis, which includes the invasion of adjacent tissues and or-

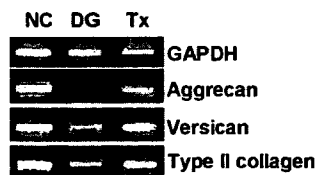
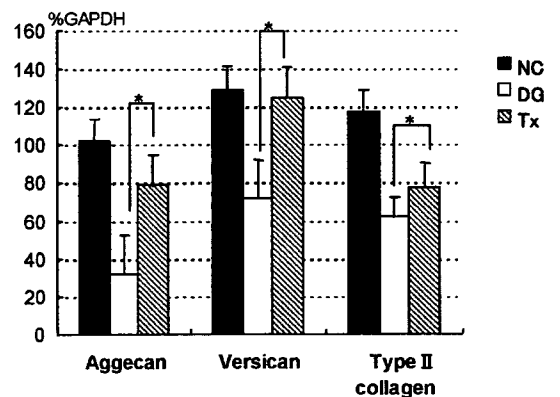


Figure 8. Results of aggrecan, versican, and Type II collagen mRNA expression showed that these matrix associated genes were significantly restored after transplantation of HNPSV-5.



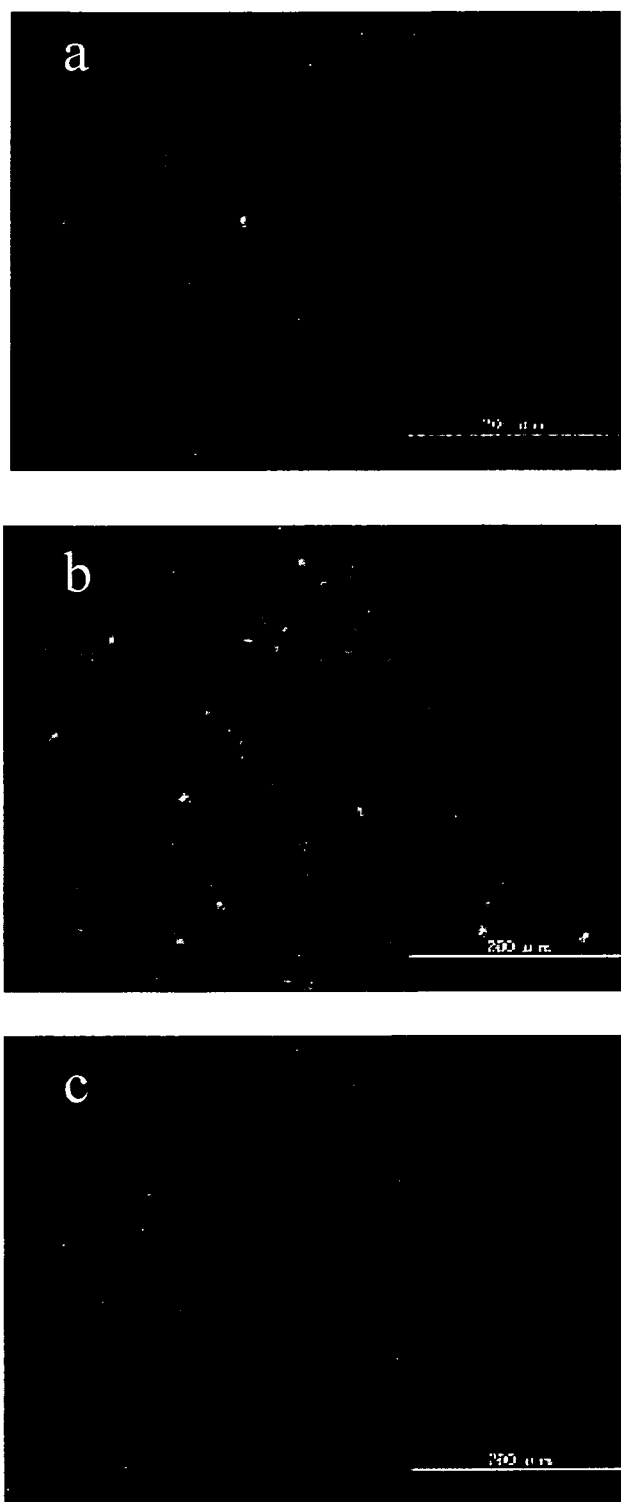


Figure 9. Cells stained positively for SV40 T antigen is seen in $89\% \pm 5\%$ of the cells in the nucleus, 24 weeks after HNPSV-5 transplantation, confirming survival of the transplanted cells. a, SV40. b, DAPI. c, SV40 + DAPI. Bars = 200 μm .

gans as well as metastasis to distant sites. Carcinogenesis is also said to require adhesion factors that are unlikely to be associated with this cell line. In this study, no obvious invasion of the AF or surrounding tissues was detected 24 weeks posttransplantation. Because the NP cells are

transplanted into an enclosed cavity surrounded by the AF and the cartilage endplate, the contact inhibition effect on the cells or a decline in the expression of SV40 T antigen may prevent tumorigenesis/carcinogenesis. Another possible reason is that metabolic activity in the NP is low and the cell cycle is prolonged.

However, some problems remain. SV40 T antigen, induced in the HNPSV cell line, is a protein that blocks the action of p53 protein and speeds the transition from G1 phase to G2 phase, possibly increasing the proportion of cells with inadequate DNA repair. The link between SV40 T antigen and telomeres, which determine the lifespan of cells, is being studied, but a definite relation has not been established.^{24,25} Studies that involve the transplantation of this cell line in immunodeficient animals, such as nude or SCID mice, are needed to examine cell differentiation and proliferation.

■ Conclusion

Several issues need to be resolved before direct clinical application of these immortalized cells can be considered, but there are no satisfactory treatments available at present for IVD degeneration and this cell line shows considerable promise as an alternative source for cell transplantation therapy because it maintains its original characteristics while showing excellent proliferation.

■ Acknowledgments

The authors thank Tomoko Nakai, Hidetoshi Inoko, and Akihiko Serizawa for expert technical assistance.

■ Key Points

- The human nucleus pulposus cell line was transplanted into rabbit discs in a disc degeneration model.
- Deceleration of disc degeneration was evident after human nucleus pulposus cell line transplantation, as shown by disc height, and macroscopic and histologic examination.
- Aggrecan and Type II collagen mRNA expression in discs from the transplanted group was significantly higher than the DG discs.
- Although further follow-up is necessary, no apparent tumorigenic activity of the transplanted cells was identified.

References

1. Gruber HE, Henry EN, et al. Analysis of aging and degeneration of the human intervertebral disc: comparison of surgical specimens with normal controls. *Spine* 1998;23:751-7.
2. Nishida K, Kang JD, Suh JK, et al. Adenovirus-mediated gene transfer to nucleus pulposus cells: implications for the treatment of intervertebral disc degeneration. *Spine* 1998;23:2437-42.
3. Walsh AJ, Bradford DS, Lotz JC, et al. In vivo growth factor treatment of degenerated intervertebral discs. *Spine* 2004;29:156-63.
4. Yoon ST, Kim SK, Li J, et al. The effect of bone morphogenetic protein-2 on rat intervertebral disc cells in vitro. *Spine* 2003;28:1773-80.

5. Masuda K, Takegami K, An H, et al. Recombinant osteogenic protein-1 upregulates extracellular matrix metabolism by rabbit annulus fibrosus and nucleus pulposus cells cultured in alginate beads. *J Orthop Res* 2003;21:922-30.
6. Kawakami M, Matsumoto T, Hashizume H, et al. Osteogenic protein (OP-1/BMP7) inhibits degeneration and pain-related behavior induced by chronically compressed nucleus pulposus in the rabbit. *Orthop Res Soc Trans* 2004;29:80.
7. Imai Y, Thonar E, Muehleman C, et al. Co-injection recombinant human osteogenic protein-1 minimizes chondroitinase ABC induced intervertebral disc degeneration: an in vivo study using a rabbit model. *Orthop Res Soc Trans* 2003;28:79.
8. Ganey T, Libera J, Moos V, et al. Disc chondrocyte transplantation in a canine model: a treatment for degenerated or damaged intervertebral disc. *Spine* 2003;28:2609-20.
9. Gruber HE, Johnson TL, Leslie K, et al. Autologous intervertebral disc cell implantation: a model using *Psammomys obesus*, the sand rat. *Spine* 2002;27:1626-33.
10. Nishimura K, Mochida J. Percutaneous reinsertion of the nucleus pulposus: an experimental study. *Spine* 1998;22:1531-39.
11. Okuma M, Mochida J, Nishimura K, et al. Reinsertion of activated nucleus pulposus cells retards intervertebral disc degeneration: an in vitro and in vivo experimental study. *J Orthop Res* 2000;18:988-97.
12. Nomura T, Mochida J, Okuma M, et al. Nucleus pulposus allograft retards intervertebral disc degeneration. *Clin Orthop* 2001;389:94-101.
13. Sakai D, Mochida J, Yamamoto Y, et al. Transplantation of mesenchymal stem cells embedded in Atelocollagen gel to the intervertebral disc: a potential therapeutic model for disc degeneration. *Biomaterials* 2003;24:3531-41.
14. Sobajima S, Kim JS, Niyibizi C, et al. Stem cell therapy for intervertebral disc diseases in vitro and in vivo feasibility study. *Orthop Res Soc Trans* 2004;29:137.
15. Crevensten G, Walsh AJ, Ananthakrishnan D, et al. Intervertebral disc therapy for regeneration: mesenchymal stem cell implantation in rat intervertebral disc. *Orthop Res Soc Trans* 2004;29:138.
16. Anderson WF, Blaes RM, Culver K, et al. The ADA human gene therapy clinical protocol: points to consider response with clinical protocol. *Hum Gene Ther* 1990;1:331-62.
17. Holm S, Nachemson AL. Variations in the nutrition of canine intervertebral disc induced by motion. *Spine* 1983;8:866-74.
18. Oemega TR Jr, et al. Biochemistry of the intervertebral disc. *Clin Sports Med* 1993;12:419-39.
19. Sakai D, Mochida J, Yamamoto Y, et al. Immortalization of human nucleus pulposus cells by a recombinant SV40 adenovirus vector. *Spine* 2004;29:1515-23.
20. Szabo G, Ragasa SJ. Changes in mRNA and protein levels of proteoglycans of the annulus fibrosus and nucleus pulposus during intervertebral disc degeneration. *Spine* 2002;27:2212-19.
21. Lu DS, Shono Y, Oda I, et al. Effects of chondroitinase ABC and chymopain on spinal motion segment biomechanics: an in vivo biomechanical, radiologic, and histologic canine study. *Spine* 1997;22:1828-34.
22. Aguiar DJ, Johnson SL, Oegema TR. Notochordal cells interact with nucleus pulposus cells: regulation of proteoglycan synthesis. *Exp Cell Res* 1999;10:246:129-37.
23. Ikeda T, Kubo T, Arai Y, et al. Adenovirus mediated gene delivery to the joints of guinea pigs. *J Rheumatol* 1998;25:1666-73.
24. Tyner SD, Venkatachalam S, Chol J, et al. p53 mutant mice that display early ageing-associated phenotypes. *Nature* 2002;415:45-53.
25. Migliaccio E, Giorgio M, Mele S, et al. The p66shc adaptor protein controls oxidative stress response and life span in mammals. *Nature* 1999;402:309-313.

厚生労働科学研究費補助金(長寿科学総合研究事業)
高齢者の腰痛症に係る効果的な診断、治療、リハビリテーション等の確立
分担研究報告書
骨粗鬆症性脊椎圧迫骨折に対する新たな低侵襲治療法の開発に関する研究
分担研究者:武政龍一 高知大学医学部整形外科 講師

研究要旨

我々は主として骨粗鬆症性椎体骨折後の偽関節または遷延治癒症例に対し、骨伝導能を有するリン酸カルシウムセメント(CPC)を用いた独自の椎体形成術を開発した。このたびその術式の安全性を保持したまま更に低侵襲化した手技として、Biportal 法を開発して臨床応用し、その有効性を検証した。本法を施行した40例44椎体(偽関節35椎体、遷延治癒9椎体)の手術時平均年齢は80歳、平均追跡期間は12ヵ月であった。1椎体あたりの平均手術時間は88分、平均術中出血は21mlと小侵襲であり、腰背部痛のVisual Analog Scale(100mm法)では、平均で術前80mmから調査時18mmに改善し、平均椎体楔状率は術前27%から調査時74%と良好に矯正されていた。術直後の安静が守れなかった1例にCPCの分節化が生じて再手術を施行したが、それ以外に神経麻痺や肺塞栓、感染などの合併症を認めなかった。椎体外漏出を2例に認めたが無症候性であった。本法は、全身麻酔を要するが高齢者でも安全に手術が施行可能であり、除痛効果と椎体変形矯正効果に優れるため、高齢者骨粗鬆症性椎体骨折の治療として有用な治療選択肢となりうる。

A. 研究目的

我々は1996年に骨伝導能を有するリン酸カルシウムセメント(CPC)を用いた独自の椎体形成術を開発し、主として骨粗鬆症性椎体骨折後に骨癒合不全となり腰背部痛が持続する偽関節または遷延治癒症例に対する治療法として用いてきた。しかし従来法では背部を6-7cm正中切開し、傍脊柱筋を棘突起から剥離する必要があり、欧米で行われている経皮的椎体形成術と比べると、椎体補強剤の漏出が少ないという安全性は確保されるものの、侵襲が増すという欠点があった。そのため、このほど安全性は従来法通りに確保しながら、より低侵襲化した新しい術式を開発した。今回その新しい低侵襲術式を臨床応用して経過観察し、その成績を調べた。

B. 研究方法

このほど開発した術式は、罹患椎体両側椎弓根上に径18mmのX線透過性円筒レトラクターを設置し、その二つのportalを介して新しく作成した専用手術器具で経椎弓根的に椎体内処置を行うBiportal法である。当科で本法を行った症例は40例44椎体(偽関節35椎体、遷延治癒9椎体)であり、発症から手術まで平均9ヵ月、手術時平均年齢は80歳、平均追跡期間は12ヵ月であった。手術時間、術中出血量、腰背部痛に対する100mm法のVisual Analog Scale(VAS)、椎体変形矯正効果を調

べる指標として椎体楔状率(椎体前縁高が後縁高に占める割合)、術後CT評価によるCPCの椎体外漏出の評価をふくめた周術期合併症の評価を行った。

(倫理面への配慮)

手術前に十分な説明をおこない、文書にてインフォームドコンセントを得た。

C. 研究結果

1椎体あたりの平均手術時間は88分、平均術中出血は21mlであった。腰背部痛のVASは、平均で術前80mmから調査時18mmに改善し、平均椎体楔状率は術前27%から調査時74%と椎体楔状変形は良好に矯正されていた。CT評価で44椎体中2椎体にCPCの椎体前側壁骨欠損部からの無症候性椎体外漏出を認めたが、隣接椎間板内や脊柱管内への漏出および経静脈性漏出は認めなかった。また、神経障害、深部感染、静脈・肺塞栓などの合併症は皆無であった。術前に高度の椎体扁平化を呈して椎体前側壁の骨欠損が著明であり、術後せん妄によりCPCが十分硬化する前に荷重した2症例にCPCのfragmentationが生じて処置椎体が再圧潰し、そのうち1例には再手術を要した。

D. 考察

全身麻酔を要し、術後CPC硬化時間の確保(72時間が推奨される)などの課題はあるが、術

直後から著明な除痛効果が得られるばかりでなく、椎体楔状変形の矯正が得られており、平均年齢が 80 歳という高齢者を対象としても重篤合併症を生じることなく手術が低侵襲性に施行できていた。

E. 結論

本法は、従来法で確立された安全性を保持しながら、より低侵襲性に除痛ならびに変形矯正効果が得られるため、高齢者の骨粗鬆症性椎体骨折、特に骨癒合不全例に対して良い適応のある有用な治療法である。

F. 研究発表

1. 論文発表

武政龍一：高齢者骨粗鬆症性椎体骨折の問題点と対策 日整会誌 80：957-969, 2006

武政龍一：骨セメント材料による骨粗鬆症性脊椎骨折の最小侵襲手術の現状と課題 バイオマテリアル 24：413-422, 2006

武政龍一、谷俊一、喜安克仁ほか：骨粗鬆症性椎体骨折に対するリン酸カルシウムセメントを用いた椎体形成術 整・災外 49：795-805, 2006

武政龍一 喜安克仁 川崎元敬ほか：骨粗鬆症性椎体骨折癒合不全の簡易な画像診断法—仰臥位側面像撮影の有用性— 中部整災誌 49：705-706, 2006

Takemasa R, Kiyasu K, Toshikazu T, et al: Diagnosis of vertebral nonunion after osteoporotic compression fractures by functional radiography: Clinical significance of lateral view in a supine position. Spine J 6:61S, 2006

武政龍一：骨粗鬆症性椎体骨折に対する椎体形成術—リン酸カルシウムセメント(CPC)を用いた修復術—日本整形外科学会企画・監修 整形外科卒後教育研修用ビデオ FXD-53, 2006

武政龍一 谷俊一 喜安克仁ほか：開創式の安全性および有効性を踏襲した小切開リン酸カルシウムセメント椎体形成術の開発 西日本脊椎研究会誌 32：182-186, 2006

武政龍一 谷俊一 喜安克仁ほか：骨粗鬆症性椎体骨折に対するリン酸カルシウムセメント椎体形成術—背筋温存小切開術式への移行— 中部整災誌 49：971-972, 2006

喜安克仁 武政龍一 谷俊一ほか：リン酸カ

ルシウム骨セメントを用いた椎体形成術—治療成績と合併症— 中部整災誌 49:961~962, 2006

Takemasa R, Tani T, Kiyasu K et al : Surgical complications and safety in mini-open transpedicular vertebroplasty using calcium phosphate cement for osteoporotic vertebral fractures Spine J 6 : 29S, 2006

喜安克仁 武政龍一 谷俊一ほか：血液と粉液比の違いがリン酸カルシウム骨セメント硬化体の圧縮強度に与える影響：椎体形成術モデルを用いた検討 Orthopaedic Ceramic Implants 25:63-66, 2006

武政龍一：高齢者に対する骨粗鬆症性椎体骨折に対するリン酸カルシウムセメントを用いた椎体形成術 脊椎脊髄 20:570-576, 2007

喜安克仁 武政龍一 谷俊一：血液存在下における注入充填方法の違いがリン酸カルシウム骨セメント硬化体の圧縮強度に与える影響—椎体形成術モデルを用いた検討— 中部整災誌 50:61~62, 2007

Takemasa R, Kiyasu K, Tani T et al. Validity of calcium phosphate cement vertebroplasty for vertebral non-union after osteoporotic fracture with middle column involvement. Spine J 7: 148S, 2007

武政龍一：椎体形成術—vertebroplasty と kyphoplasty— 日脊会誌 18: 2007 in press

2. 学会発表

Takemasa R, Kiyasu K, Toshikazu T, et al: Diagnosis of vertebral non-union after osteoporotic compression fractures by functional radiography: Clinical significance of lateral view in a supine position. 33rd Annual meeting of international society for the study of lumbar spine in Bergen 2006

Takemasa R, Tani T, Kiyasu K et al : Surgical complications and safety in midline mini-open vertebroplasty using calcium phosphate cement for osteoporotic vertebral fractures 33rd Annual meeting of international society for the study of lumbar spine in Bergen 2006

Takemasa R, Kiyasu K, Toshikazu T, et al: Diagnosis of vertebral non-union after

osteoporotic compression fractures by functional radiography : Clinical significance of lateral view in a supine position. North American Spine Society 21st annual meeting in Philadelphia 2006

Takemasa R, Tani T, Kiyasu K et al : Surgical complications and safety in mini-open transpedicular vertebroplasty using calcium phosphate cement for osteoporotic vertebral fractures North American Spine Society 21st annual meeting in Philadelphia 2006

Takemasa R Verbroplasty using calcium phosphate cement(CPC) —specific surgical technique and clinical results — Catholic international neurosurgery update in Soul, 2007-11-26

Takemasa R, Kiyasu K, Tani T et al. Validity of calcium phosphate cement vertebroplasty for vertebral non-union after osteoporotic fracture with middle column involvement. North American Spine Society 22nd annual meeting in Austin 2007

武政龍一 喜安克仁 川崎元敬ほか 骨粗鬆症性椎体骨折骨癒合不全の簡易な画像診断法—仰臥位側面像撮影の有用性— 第 106 回中部日本整形災害外科学会

武政龍一 谷俊一 喜安克仁ほか 骨粗鬆症性椎体骨折に対するリン酸カルシウムセメント椎体形成術—背筋温存小切開術式への移行— 第 106 回中部日本整形災害外科学会

武政龍一 谷俊一 喜安克仁ほか 骨粗鬆症性椎体骨折に対するリン酸カルシウムセメントを用いた椎体形成術—開窓術式から小切開背筋温存式への術式転換—第 35 回日本脊椎脊髄病学会 2006

骨粗鬆症性椎体骨折に対する買い開創式リン酸カルシウム骨セメント椎体形成術における安全性の検証 武政龍一 谷俊一 喜安克仁ほか 第 35 回日本脊椎脊髄病学会 2006

武政龍一 谷俊一 喜安克仁ほか 脊髄・馬尾への圧迫を有する胸腰椎移行部骨粗鬆症性椎体圧潰に対する椎体形成術を併用した後方進入再建術 第 35 回日本脊椎脊髄病学会 2006

武政龍一 谷俊一 喜安克仁ほか 骨粗鬆症性椎体骨折に対するリン酸カルシウム骨セメント椎体内注入術の合併症 第 79 回日本整形外科学会学術集会 2006

武政龍一 喜安克仁 谷俊一 血液存在下における注入充填法法の違いがリン酸カルシウム骨セメント硬化体の圧縮強度に与える影響—椎体形成術モデルを用いた検討—第 35 回日本脊椎脊髄病学会 2006

武政龍一 骨粗鬆症性椎体骨折に対する最小侵襲手術—リン酸カルシウムセメントを用いた椎体形成術の実際とピットフォール— 第 21 回日本脊髄外科学会特別講演 2006

武政龍一 リン酸カルシウムペーストを用いた椎体形成術—低侵襲性と安全性確保のための工夫— 第 13 回日本脊椎・脊髄神経手術手技学会 2006

武政龍一 リン酸カルシウムペーストを用いた椎体形成術の手術手技 ワークショップ第 13 回日本脊椎・脊髄神経手術手技学会 2006

喜安克仁 武政龍一 谷俊一ほか 単純 X 線機能撮影による骨粗鬆症性椎体骨折癒合不全の診断—仰臥位側面像撮影の有用性について—第 35 回日本脊椎脊髄病学会 2006

喜安克仁 武政龍一 谷俊一 椎体形成術モデルにおけるリン酸カルシウム骨セメントの圧縮強度—血液と粉液比の影響について—第 35 回日本脊椎脊髄病学会 2006

喜安克仁 武政龍一 谷俊一ほか 単純 X 線機能撮影による骨粗鬆症性椎体骨折癒合不全の診断—仰臥位側面像撮影の有用性について—第 79 回日本整形外科学会学術総会 2006

喜安克仁 武政龍一 谷俊一ほかリン酸カルシウム骨セメントを用いた椎体形成術—治療成績と合併症—第 106 回中部日本整形災害外科学会 2006

喜安克仁 武政龍一 谷俊一 リン酸カルシウム骨セメント充填方法の違いが硬化体圧縮強度に与える影響—椎体形成術モデルを用いた検討—第 106 回中部日本整形災害外科学会

喜安克仁 武政龍一 井上真輔ほか 椎体後壁損傷を伴う骨粗鬆症性椎体骨折癒合不全に対する椎体形成術 第 107 回中部日本整形災害外科学会 2006

喜安克仁 武政龍一 谷俊一 骨粗鬆症性椎体圧迫骨折後偽関節に対する椎体形成術の椎体楔状変形矯正効果 第 40 回日本側弯症学会 2006

武政龍一 谷俊一 喜安克仁ほか 高齢者骨粗鬆症性椎体骨折癒合不全に対する安全か

つ侵襲の少ない椎体形成術 第108回中部日本整形災害外科学会 2007

武政龍一 喜安克仁 谷俊一ほか 椎体後壁破綻を伴う骨粗鬆症性椎体骨折後骨癒合不全に対するリン酸カルシウムセメントを用いた椎体形成術 第 36 回日本脊椎脊髄病学会 2007

武政龍一 谷俊一 川崎元敬ほか 骨補填材としてのリン酸カルシウム骨セメントにおける課題 第 80 回日本整形外科学会学術集会パネルディスカッション 2007

武政龍一 腰痛の病態と対策 第40回中国四国整形外科学会教育研修講演 2007

喜安克仁 武政龍一 谷俊一 リン酸カルシウム骨セメント充填方法の違いが硬化体圧縮強度に与える影響—椎体形成術モデルを用いた検討—第22回日本整形外科基礎学術集会 2007

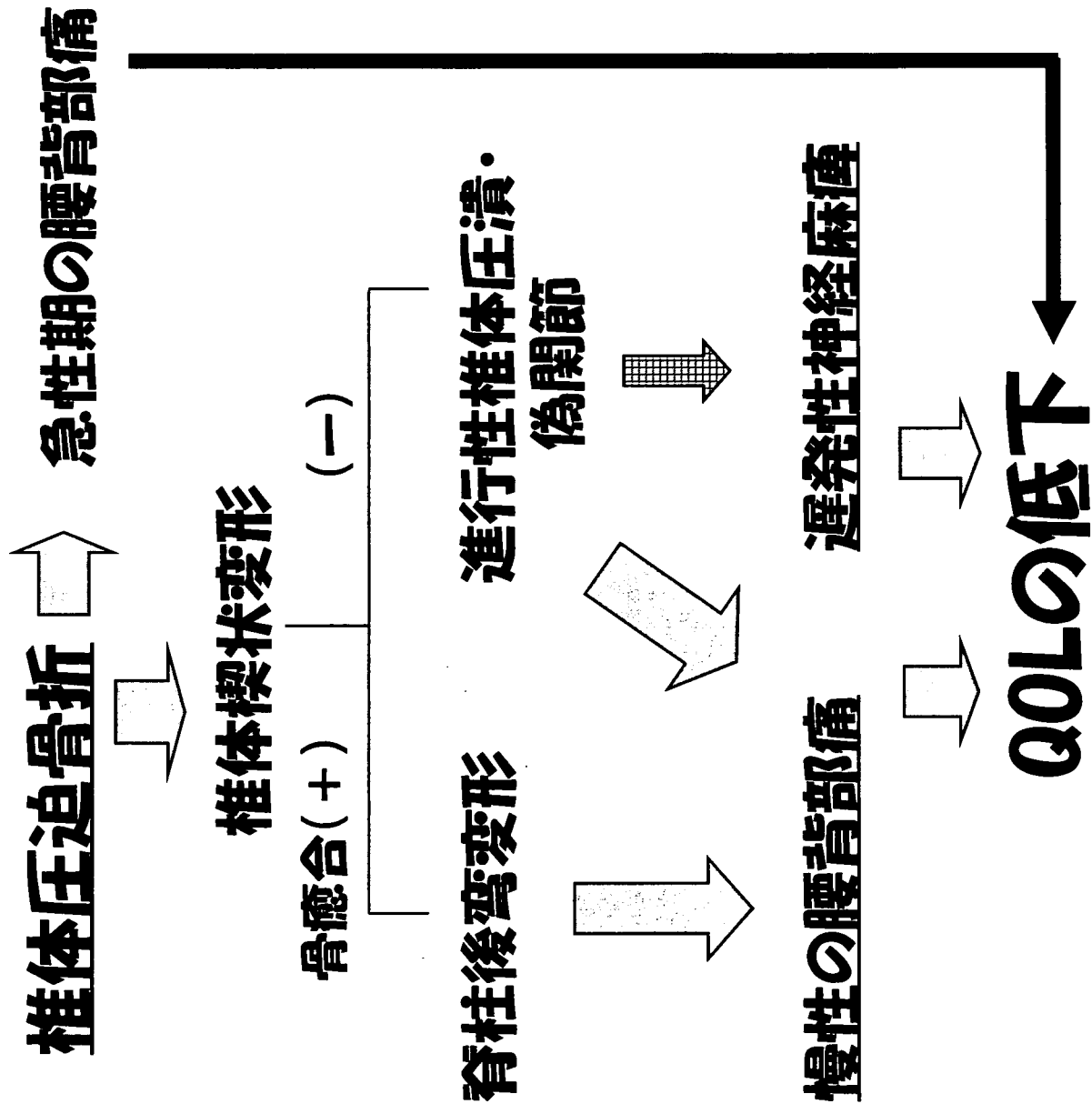
G.知的財産権の出願・登録状況

1. 意匠登録

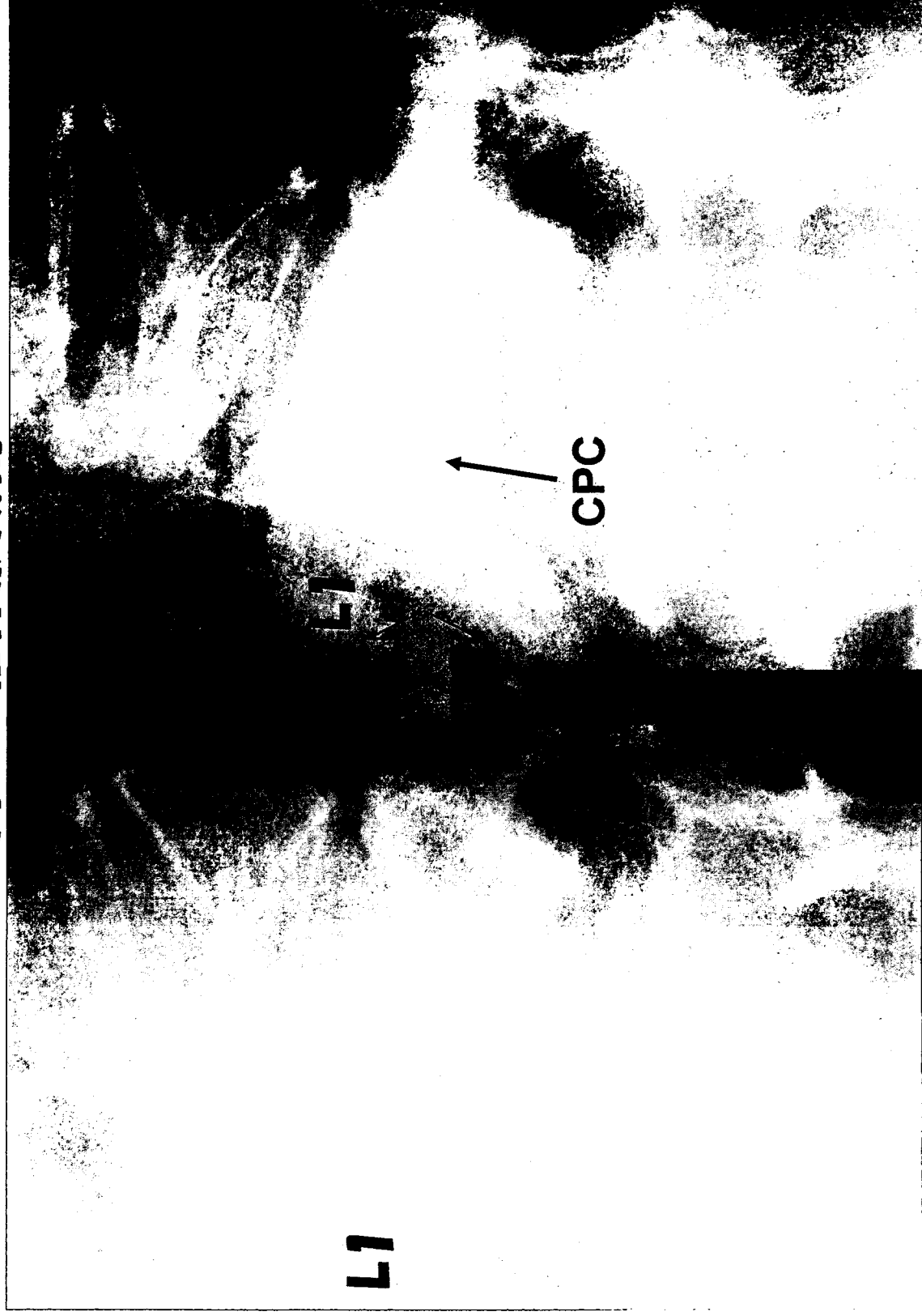
登録第 1301335 号 椎体内キュレット
2007.4.13

登録第 1301336 号 椎体内ラスプ 2007.4.13

骨粗鬆症性椎体圧迫骨折



椎体骨折後骨癒合不全例に対する
リン酸カルシウムセメント(Calcium Phosphate Cement : CPC)
を用いた椎体形成術

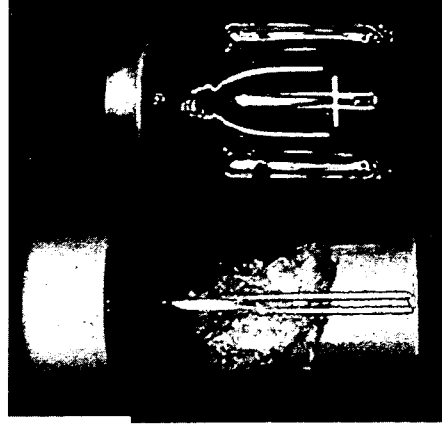


術前

術後

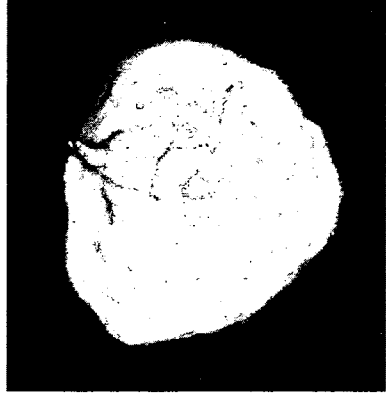
Calcium Phosphate Cement(CPC)

injectable paste



粉体 溶解液

α -TCP



練和

HA

水和反応

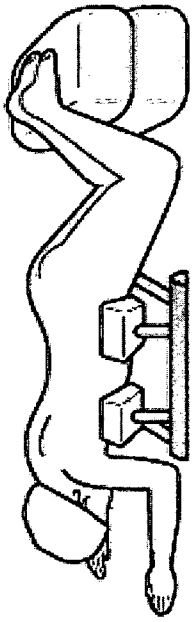
(非発熱性)

■ 圧縮強度: 80MPa

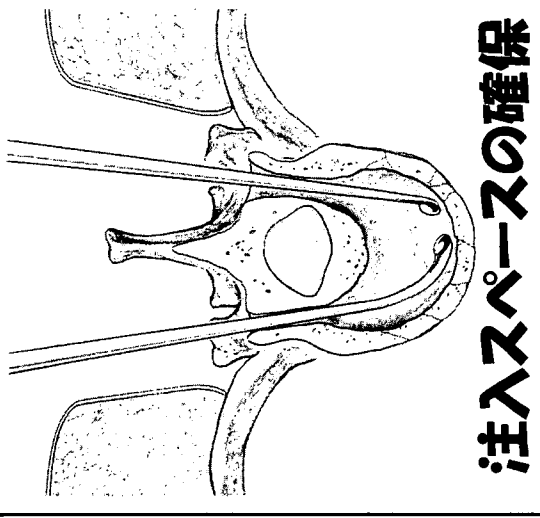
■ 生体活性

■ 骨伝導能

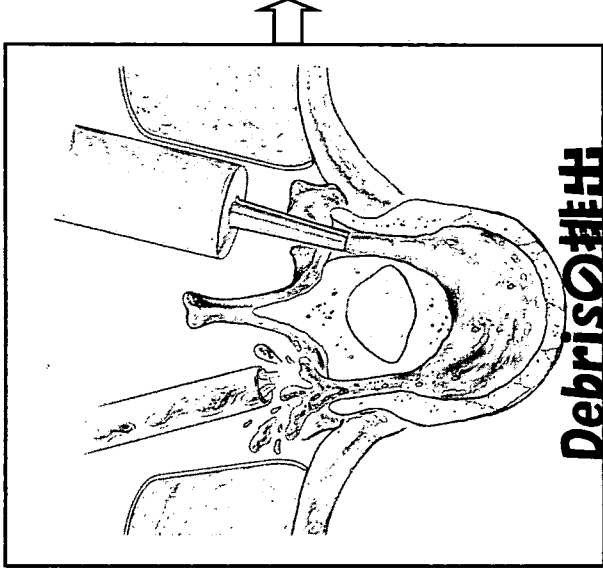
正中切開術式によるCPC椎体形成術: 96例110椎体 (全身麻酔下6cm正中切開)



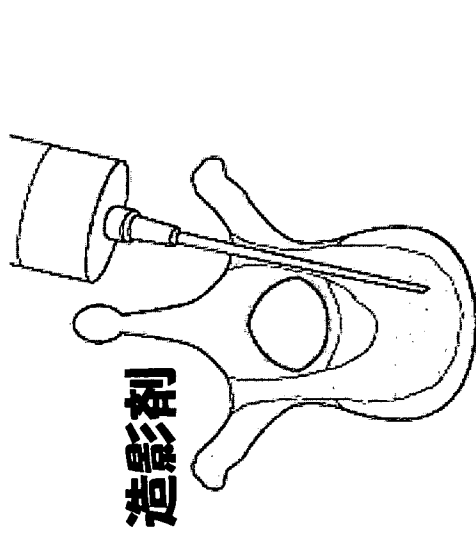
椎体変形の整復



注入スペースの確保

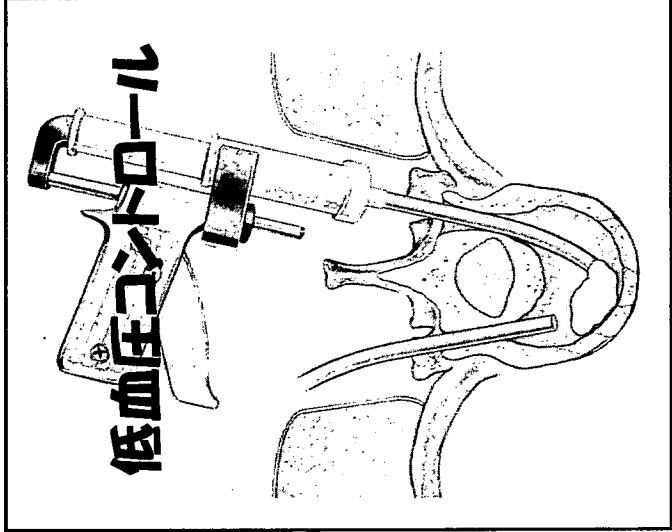


Debrisの排出



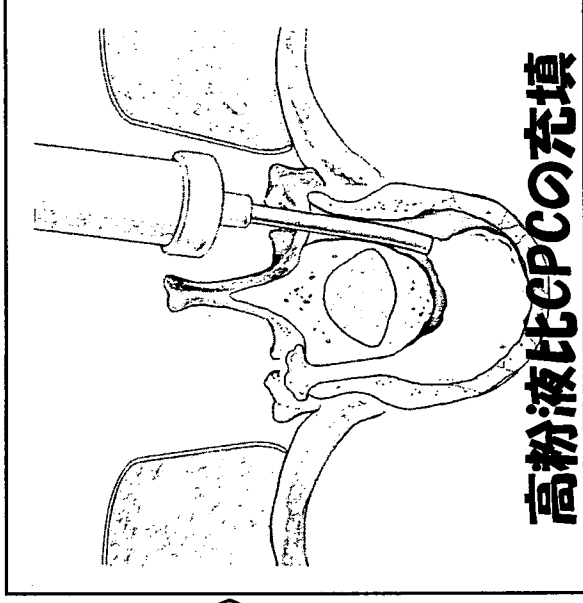
造影剤

造影剤で漏れのチェック



低血圧コントロール

貯留液の吸引|排出

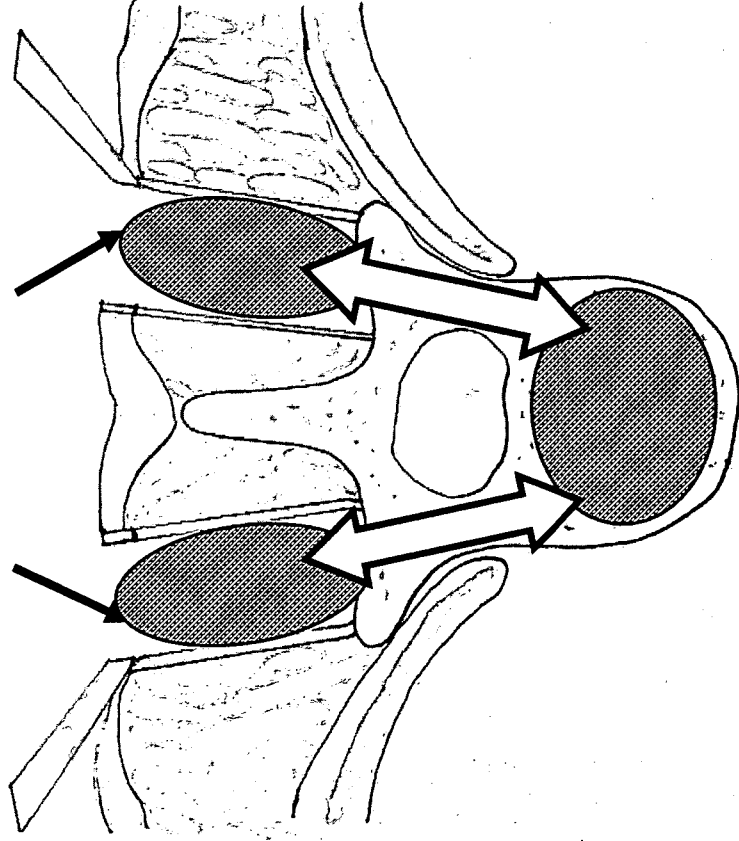


高粉液比CPCの充填

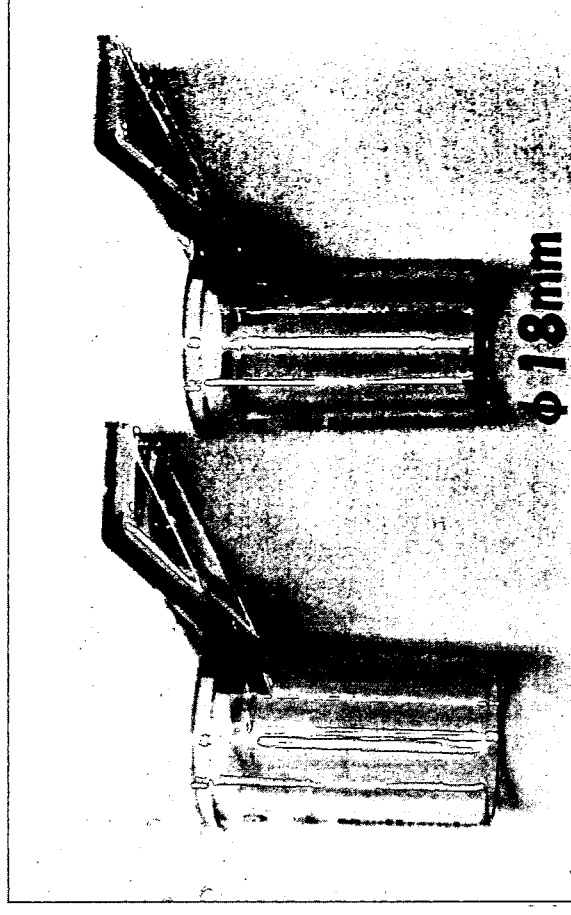
Biportal technique

シトクター内空間を
減圧腔および作業空間として利用

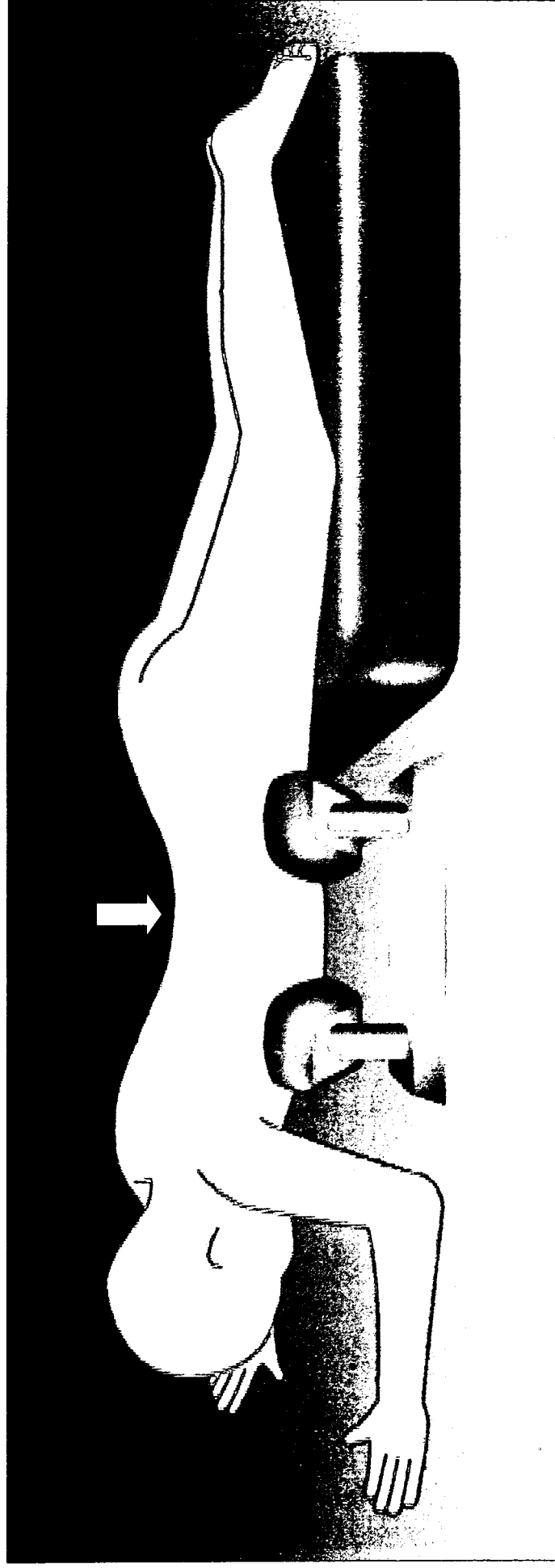
X線透過性円筒シトクター



X線透過性円筒シトクター



Surgical Procedure (1)



椎体楔状変形を矯正

